Available online at www.sciencedirect.com

ScienceDirect

Russian Geology and Geophysics 58 (2017) 744–751

RUSSIAN GEOLOGY AND GEOPHYSICS

www.elsevier.com/locate/rgg

Wave transforms of transient electromagnetic field in conductive earth

G.A. Gretskov [a,*], M.I. Epov [a,b], E.Yu. Antonov [a]

[a] *A.A. Trofimuk Institute of Petroleum Geology and Geophysics, Siberian Branch of the Russian Academy of Sciences, pr. Akademika Koptyuga 3, Novosibirsk, 630090, Russia*

[b] *Novosibirsk State University, ul. Pirogova 2, Novosibirsk, 630090, Russia*

Received 19 April 2016; accepted 1 September 2016

Abstract

The study aims at finding a stable method for transformation of time-domain electromagnetic diffusion field to an electromagnetic wavefield. Two ways of transformation are considered: singular-value decomposition (SVD) and Tikhonov's regularizations. Transformation is applied to TEM responses of a conductive half-space, a conductive *S* film, and to a series of horizontally layered models. The wave transforms are used to plot travel-time curves and to estimate the velocity of EM field propagation.

Keywords: TEM soundings; wave transform; regularization

Introduction

The use of transient electromagnetic soundings since the late 1950s–early 1960s, first in the far-field (Van'yan, 1963) and then in the near-field (Kaufman and Morozova, 1970) modifications, has contributed a lot to progress of resistivity surveys. A similar method based on the transient process came in use in mineral exploration (Kamenetsky, 1997). The theory of transient electromagnetic fields was developed, for instance, in studies by Van'yan (1965) and Sheinmann (1969). The transmitters of TEM signals have the form of current loops or grounded lines (not considered in this paper). The turn-off of transmitter current at some time induces eddy currents in conductive subsurface according to the Farady law, in the quasi-stationary approximation (Kaufman and Morozova, 1970). The eddy currents propagate depthward and decay at rates controlled by energy loss and earth's resistivity, which allows discriminating between conductive and resistive rocks. The data acquissition system records electromotive force (voltage) induced in the receiver loop or the potential difference between closely spaced receiver electrodes (not considered below). Thus, TEM systems most often consist of a transmitter and several receiver loops of which one is placed in the center of the transmitter (central-loop configuration) while others may lie either inside or outside the transmitter loop. Each receiver records time-dependent voltage decay (TEM responses). For convenience of analysis, the measured values are converted into apparent values of resistivity ρ_τ, conductivity s_τ and depth h_τ (Sidorov, 1985). The measured data are inverted to parameters of rocks, but inversion is a labor-consuming process, even with reference to a simple horizontally layered starting model, especially if multiple sources and receievrs are used.

The gained experience of TEM data processing and interpretation, as well as success in seismic exploration, have demonstrated that imaging the true resistivity structure of the subsurface requires using greater number of receivers and transmitters. In this respect, systems of seismic surveys, with a bunch of regularly arranged receivers recording responses to a single shot, can be used as example. A similar system for TEM surveys considered in this paper may comprise a square transmitter loop and multiple equally spaced receivers placed along a line, with the first receiver centered at the transmitter center (central-loop configuration). Thus acquired data can be processed and interpreted in the same way as seismic data (Nekut, 1994; Virieux et al., 1994; Yu and Edwards, 1997). Propagation of waves from seismic and electromagnetic sources is described, respectively with the wave equation and with the equations of diffusion or thermal conductivity, assuming quasi-stationary conditions (Kaufman and Morozova, 1970). Therefore, the use of processing techniques similar to those in seismic surveys requires transformation of the diffusion EM field into the wave field (Lee et al., 1989; Zhdanov and Frenkel, 1983).

* Corresponding author.
E-mail address: greckov.gleb@gmail.com (G.A. Gretskov)

1068-7971/$ - see front matter
http://dx.doi.org/10.1016/j.rgg.2016.09.031

This transformation is possible by mapping the space of the diffusion equation solutions onto that of wave equation solutions using the Laplace transformation (Kunetz, 1972; Reznitskaya, 1974; Weidelt, 1972). However, the numerical implementation of the approach is problematic because of instability and uncertainty. Instability is caused by the exponential kernel of the Laplace transform and can be overcome by regularization with various methods. For instance, Lee and Xie (1993) apply ray tomography to low-frequency Controlled Source ElectroMagnetic (CSEM) data by transforming a diffusive EM field to a wavefield defined in a time-like variable mathematically using singular-value decomposition. This approach leads to some useful results, but the obtained wave signals oscillate strongly and are unfit for processing by the methods for seismic data. Levy et al. (1988) provide the stability of the transform by minimizing the linear programming norm L_1. Other attempts to acvhieve stability in transforming the solutions for diffusive fields into those for wavefields (Gershenson, 1997; Gibert and Virieux, 1991; Slob et al., 1995; Wilson, 1994) mainly use field decomposion into implusive functions which can be transformed analytically. All these methods stem from numerical stability and take no acccount of the desirable physical properties of the resulting wave transforms. Regularization of integral transformation was considered in detail by Swidinsky (2011) who applied Tikhonov's SVD regularization (Tikhonov and Arsenin, 1979) with different parameters to CSEM data. Methods of CSEM data processing similar to those for seismic data were also reported by Mittet (2015), while Xie et al. (2012) suggested regularization for transformation of the diffusion equation into the wave equation for TEM data.

Theoretical background

Propagation of the electromagnetic field in a homogeneous and isotropic conductive earth with the dielectric pemittivity ε_0, magnetic permeability μ_0 and electrical conductivity σ, in the absence of additional sources, is described by a system of Maxwell equations, using the time-dependent (t) electric field vector $\mathbf{E}$ and magnetic flux $\mathbf{B}$ in the coordinates x, y, z:

$$\nabla \times \mathbf{B} = \mu_0 \sigma \mathbf{E} + \mu_0 \varepsilon_0 \frac{\partial \mathbf{E}}{\partial t}, \quad (1)$$

$$\nabla \times \mathbf{E} = -\frac{\partial \mathbf{B}}{\partial t}, \quad (2)$$

$$\nabla \cdot \mathbf{E} = 0, \quad (3)$$

$$\nabla \cdot \mathbf{B} = 0. \quad (4)$$

The first and second terms in the right-hand part of equation (1) refer, respectively, to conduction and eddy (displacement) currents; the latter is assumed below to be much smaller than the former, according to the quasi-stationary conditions (Kaufman and Morozova, 1970), and thus negligible. Then the diffusion equation is obtained applying rotation to (1) and (2), neglecting the eddy current, and using the vector analysis equation $\nabla \times \nabla \times A = \nabla(\nabla A \cdot A) - \nabla^2 A$. In the Cartesian coordinates x, y, z, it is

$$\nabla^2 \mathbf{B} = \mu_0 \sigma \frac{\partial \mathbf{B}}{\partial t}, \quad (5)$$

$$\nabla^2 \mathbf{E} = \mu_0 \sigma \frac{\partial \mathbf{E}}{\partial t}. \quad (6)$$

Assume further that some vector fields $\mathbf{F}$ and $\mathbf{G}$ depend on the variable q, as well as on the same spatial coordinates x, y, z, and are chosen such to satsify the system

$$\nabla \times \mathbf{F} = \frac{1}{\psi^2} \frac{\partial \mathbf{G}}{\partial q}, \quad (7)$$

$$\nabla \times \mathbf{G} = -\frac{\partial \mathbf{F}}{\partial q}, \quad (8)$$

$$\nabla \cdot \mathbf{F} = 0, \quad (9)$$

$$\nabla \cdot \mathbf{G} = 0. \quad (10)$$

Rotation of (7) and (8), with the above vector equation, leads to

$$\nabla^2 \mathbf{F} = \frac{1}{\psi^2} \frac{\partial^2 \mathbf{F}}{\partial q^2}, \quad (11)$$

$$\nabla^2 \mathbf{G} = \frac{1}{\psi^2} \frac{\partial^2 \mathbf{G}}{\partial q^2}. \quad (12)$$

Expressions (11) and (12) are wave equations for the fields $\mathbf{F}$ and $\mathbf{G}$ with the velocity ψ. Any fileds that satisfy equations (11) and (12) can be processed with the same methods as for seismic waves.

The transformation of the electromagnetic fileds $\mathbf{E}$ and $\mathbf{B}$ that satisfy the system of equations (1)–(4) into the wave fields $\mathbf{F}$ and $\mathbf{G}$ that satisfy a system equivalent to (7)–(8) was discussed in some theoretical studies (Hoop, 1996; Swidinsky, 2011). The transoformation into the wave domain can be obtained from equations (1) and (2), with the term $\mathbf{M}$ responsible for eddy currents at the source:

$$\nabla \times \mathbf{B} = \mu_0 \sigma (x, y, z) \mathbf{E} + \mathbf{M}, \quad (13)$$

$$\nabla \times \mathbf{E} = -\frac{\partial \mathbf{B}}{\partial t}. \quad (14)$$

Equations for the wave fields $\mathbf{F}$ and $\mathbf{G}$ are obtained with the source function (the term $\mathbf{K}$) added to (7) and (8):

$$\nabla \times \mathbf{F} = \frac{1}{\psi (x, y, z)^2} \frac{\partial \mathbf{G}}{\partial q} + \mathbf{K}, \quad (15)$$

$$\nabla \times \mathbf{G} = -\frac{\partial \mathbf{F}}{\partial q}. \quad (16)$$

Swidinsky (2011) reported transformation of the solution to (1)–(4) into that for a system equivalent to (7)–(8). The formalism for a symmetrical system of Maxwell equations with a fictitious magnetic charge added as a field source can be found in (Hoop, 1996). A pair of diffusion-to-wave transforms is obtained by the Laplace transformation as

$$\mathbf{B}(t) = \int_0^\infty W_1(t, q)\,\mathbf{F}(q)\,dq \tag{17}$$

and

$$\mathbf{E}(t) = \int_0^\infty W_2(t, q)\,\mathbf{G}(q)\,dq, \tag{18}$$

where

$$W_1(t, q) = \frac{1}{\sqrt{4\pi t^3}}\sqrt{\alpha}\; q \exp\left(-\frac{\alpha q^2}{4t}\right),$$

$$W_2(t, q) = \frac{1}{\sqrt{4\pi\alpha t}}\left[\frac{\alpha q^2}{2t} - 1\right]\exp\left(-\frac{\alpha q^2}{4t}\right).$$

The parameter α in the equations for W_1 and W_2 is the scaling coefficient of the time variable (hereafter called 'noncalibrated time').

In some specific cases, transformations (17) and (18) are possible in the analytical way, but numerical methods are applied most often to real data.

With discretization at an equal stepsize Δt in time and at Δq in pseudotime, the electromagnetic field is written as the vectors **E** and **B** of the length N, with their elements being electric and magnetic fields calculated within the specified time count. In the same way, the pseudowave fields can be written as the vectors **F** and **G** of the length **M**, with elements calculated for the specified value q. From equations (16) and (17) it is clear that integration is performed over a semiinfinite interval, but finite lengths of the vectors **M** and **N** are required for the numerical case.

After discretization, integral equations (17) and (18) with respect to the functions **F** and **G** can be written in the matrix form:

$$\hat{A}_1\,\mathbf{F} = \mathbf{B}, \tag{19}$$

$$\hat{A}_2\,\mathbf{G} = \mathbf{E}. \tag{20}$$

The exponentially decaying kernel of the transform in $W_1(t, q)$ at a quite large argument q and a small argument t leads to exponential zeroing of the singular numbers $\hat{A}_1$. Such matrices, with a great number of nearly zero elements are quasi-degenerated, and back transformation from the diffusion domain to the wave domain is thus unstable. Solving such ill-posed problems is possible with regularization by various methods.

Numerical transformation

Equation (19) for the vector **F** can be solved (Swidinsky, 2011) using singular-value decomposition (SVD) of the matrix $\hat{A}_1$ leading to the dot product of three matrices:

$$\hat{A}_1 = \hat{U}\hat{L}\hat{V}^T,$$

where

$$\hat{U}^T\hat{U} = \hat{V}^T\hat{V} = \hat{V}\hat{V}^T = \hat{I},$$

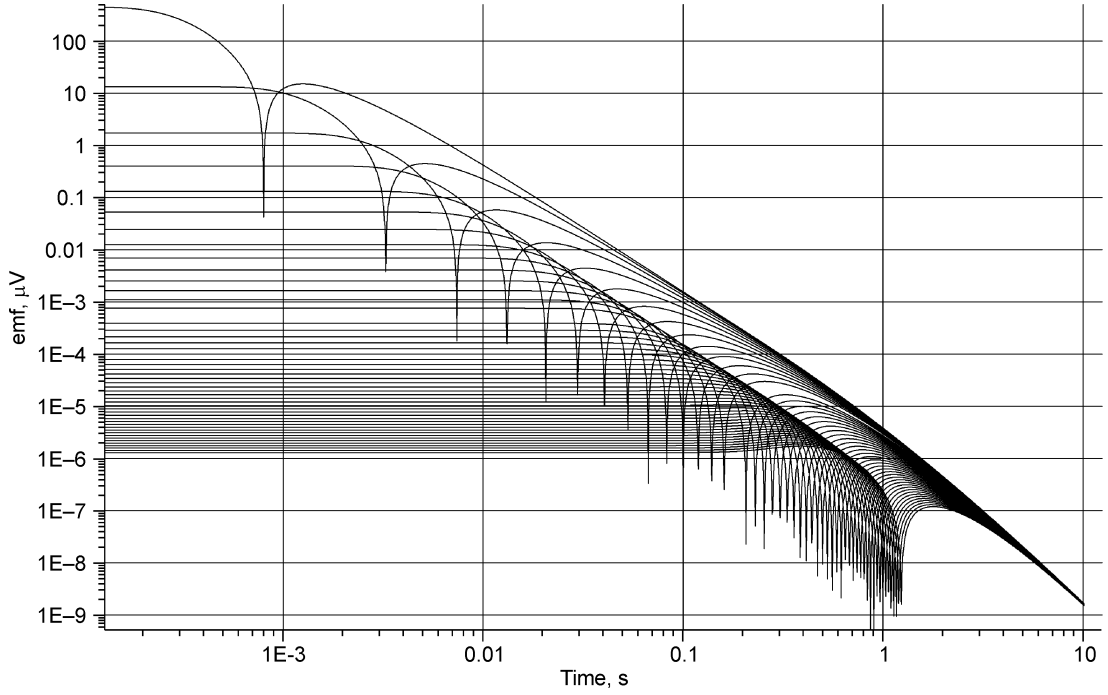

Fig. 1. Transient responses of a multioffset system.

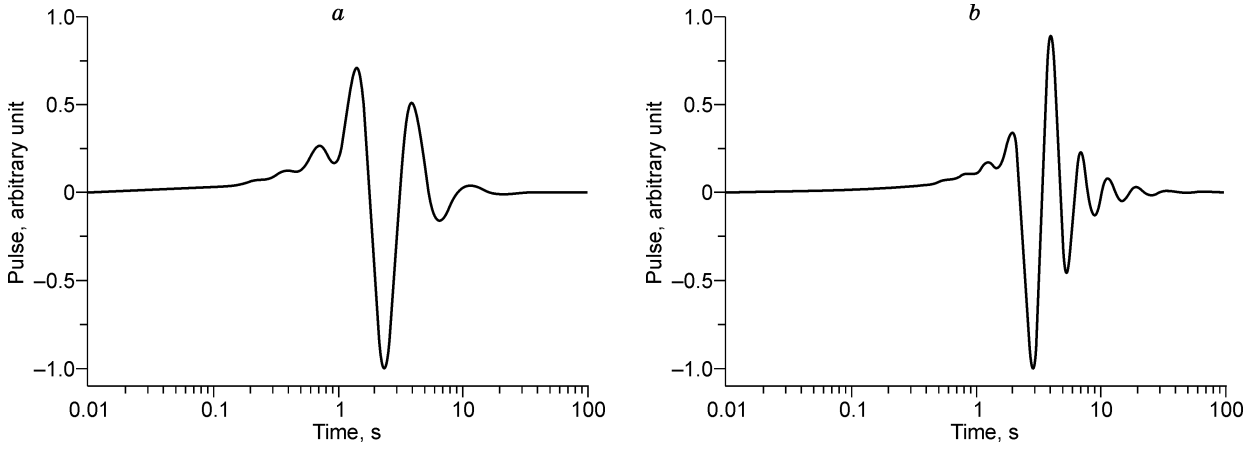

Fig. 2. Wave transform obtained using SVD (r = 4400 m) (*a*) and Tikhonov's (r = 4400 m) regularizations (*b*).

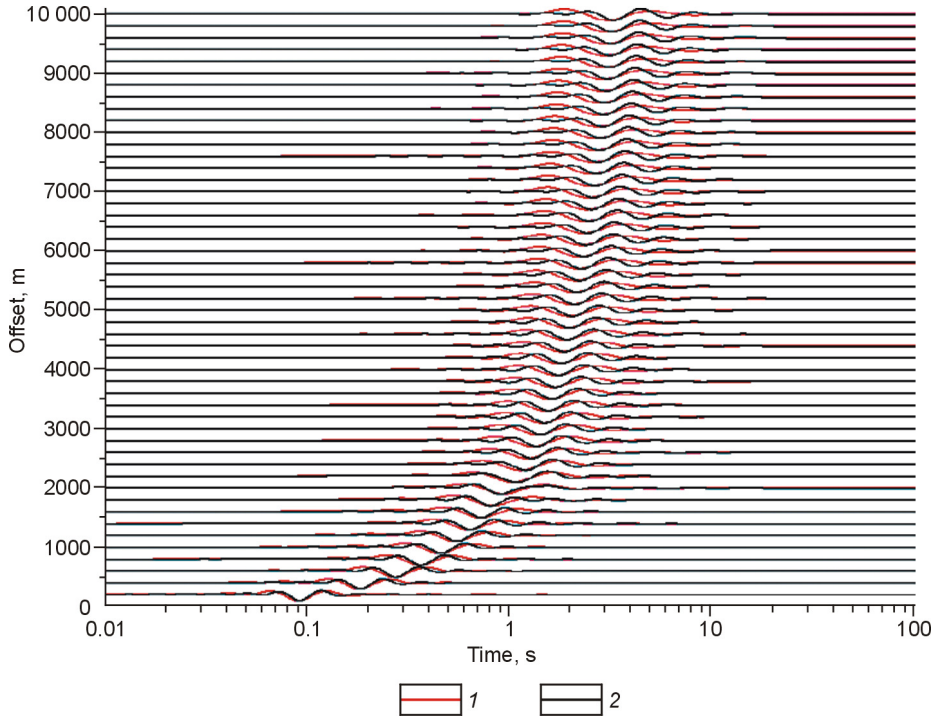

Fig. 3. Comparison of wave transforms obtained using SVD (*1*) and Tikhonov's regularizations (*2*).

where $\hat{I}$ is a unit matrix, and the matrix $\hat{L}$ contains singular values of the matrix $\hat{A}_1$ on its main diagonal. Then the non-regularized solution $\mathbf{F}$ can be written as

$$\mathbf{F} = \hat{V}\hat{L}^{-1}\hat{U}^{T}\mathbf{B}. \quad (21)$$

Solution to (21) is numerically unstable because the singular values of the quasi-degenerated matrix $\hat{A}_1$ are vanishing, but it can become stable if the regularization parameter k is added to these values:

$$\mathbf{F} = \hat{V}(\hat{L}^{2} + k\hat{I})^{-1}\hat{L}\hat{U}^{T}\mathbf{B}. \quad (22)$$

Otherwise, Tikhononv's regularization (Tikhonov and Arsenin, 1979) can be applied to stabilize the solution of (19). With the regularization Γ, the solution becomes

$$\mathbf{F} = \hat{A}_1^{T}\hat{W}\hat{A}_1 + \lambda\hat{\Gamma}^{T}\hat{\Gamma})^{-1}\hat{A}_1^{T}\hat{W}\mathbf{B}, \quad (23)$$

where λ is the regularization parameter and $\hat{W}$ is the diagonal matrix bearing calculation errors.

The transformation into the wave domain can be performed numerically using the model of a layered conductive half-space with two plane-parallel boundaries (model 1: ρ_1 = 10 Ohm·m, h_1 = 1000 m; ρ_2 = 200 Ohm·m, h_2 = 2500 m; ρ_3 = 1000 Ohm·m, ρ is the layer resistivity, and h is the layer

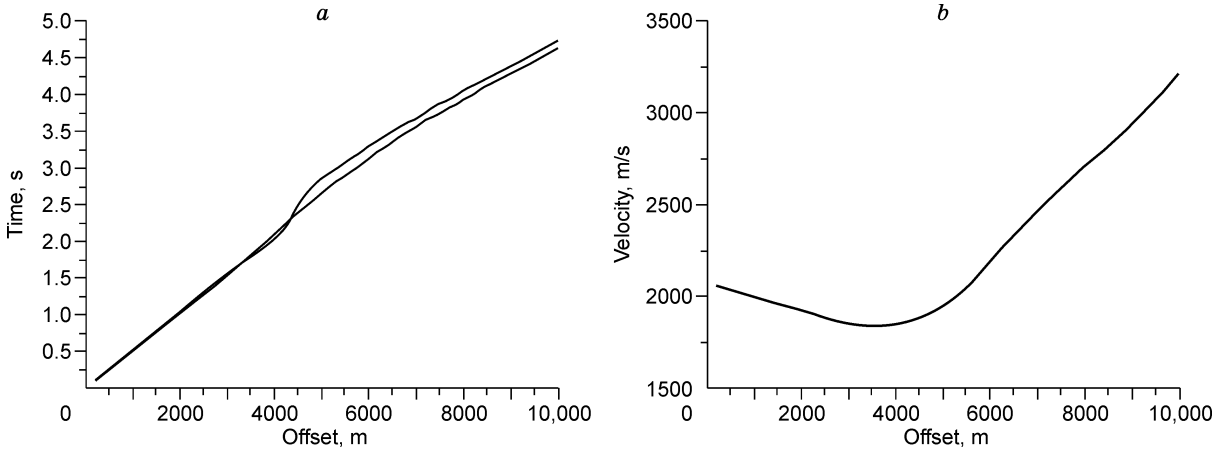

Fig. 4. Travel time (*a*) and velocity (*b*) curves based on wave transforms for a three-layer earth.

thickness), lying under a nonconductive half-space. The source has a form of a square transmitter loop, with a unit current, lying on the flat surface of the conductive half-space. The transmitter current is turned-off instantaneously at the time $t = 0$:

$$J(t) = \begin{cases} 1, & t < 0; \\ 0, & t \geq 0. \end{cases} \tag{24}$$

The induced emf (voltage) is measured by square receiver loops placed at equal spacing along a profile on the extension of one transmitter axis. Curves of time-dependent voltage decay $\varepsilon(t)$ (Fig. 1) for a set of offsets (distance between the transmitter and receiver centers) at different points of the profile are described as solutions to the diffusion equation.

Further two above numerical algorithms are used for the transformation of the multiple-offset $\varepsilon(t)$ into the wave field **F** (17). The number of time counts is $N = 3200$; the time t is specified with a uniform stepsize from 0.0001 s to 10 s; $M = 2400$; q changes with a constant step of 0.01 s to 100 s; the scaling coefficient is $\alpha = 0.5$; the parameter k for SVD regularization after a number of numerical experiments is assumed to be 10^{-4}. The regularization is performed with the unit matrix $\hat{\Gamma}_{\text{norm}}$, and the parameter λ is likewise assumed to be 10^{-4}. Numerical solution to (22) and (23) for the sets of curves $\varepsilon(t)$ leads to the wave field **F**. Figures 2*a* and 2*b* show, respectively, the wave transforms obtained by the SVD method (offset $r = 4400$ m) and by Tikhonov's regularization.

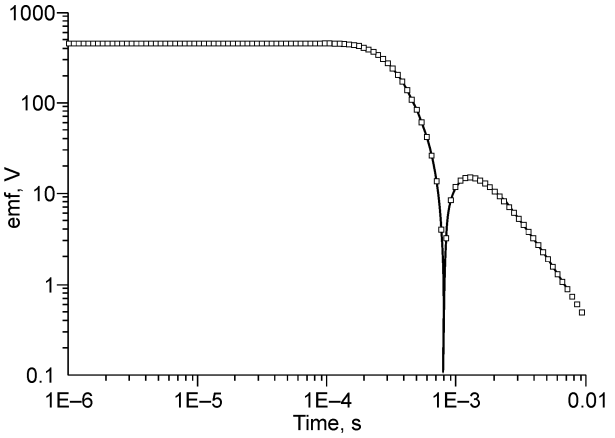

Fig. 5. Test of mutual uniqueness of wave transforms: original voltage decay curve (solid line) and voltage decay curve obtained by wave transform inversion (white circles).

The wave transforms obtained by different regularization methods for all offsets (Fig. 3) are used then to plot offset dependence of travel times (Fig. 4*a*). The travel time curves for some typical geological sections can be obtained as follows. Note that the travel times for the cases of SVD and Tikhonov's regularizations are quite similar (Fig. 4*a*). That for Tikhonov's regularization shows more distinct boundary effects in the distance range 1600–2400 m while that for SVD is smoother. The match of travel time curves can be achieved by fitting the regularization parameters but the SVD regularization is simpler. Therefore, the SVD regularization is applied further for solving equation (17). The travel-time curves can be used to calculate the velocity of the wave transform $v = 1/(\partial t/\partial r)$; the respective velocity variations are shown in Fig. 4*a*.

In order to test the transformation into the wave equation solutions, the wave transform ($r = 200$ m) is substituted into the right-hand part of equation (17). The resulting TEM curve differs slightly from the original voltage decay curve (Fig. 5): relative deviation does not exceed 1.5% before 0.01 s and then increases with time, but the late-time tail of the curve (after 0.1 s) is impossible to reconstruct.

The travel-time curves for the conductive half-space with different resistivities (Fig. 6*a*) show that the slope decreases with resistivity increase. The respective velocities (Fig. 6*b*) remain the same for all offsets and for all resistivity values: 2230 m/s at $\rho = 10$ Ohm·m, increasing with resistivity to 4973 m/s at $\rho = 50$ Ohm·m; the velocity ratio is $v_1/v_2 = \sqrt{\rho_1/\rho_2}$.

As another example, consider emf induced by a vertical magnetic dipole with the moment M above an infinitely thin

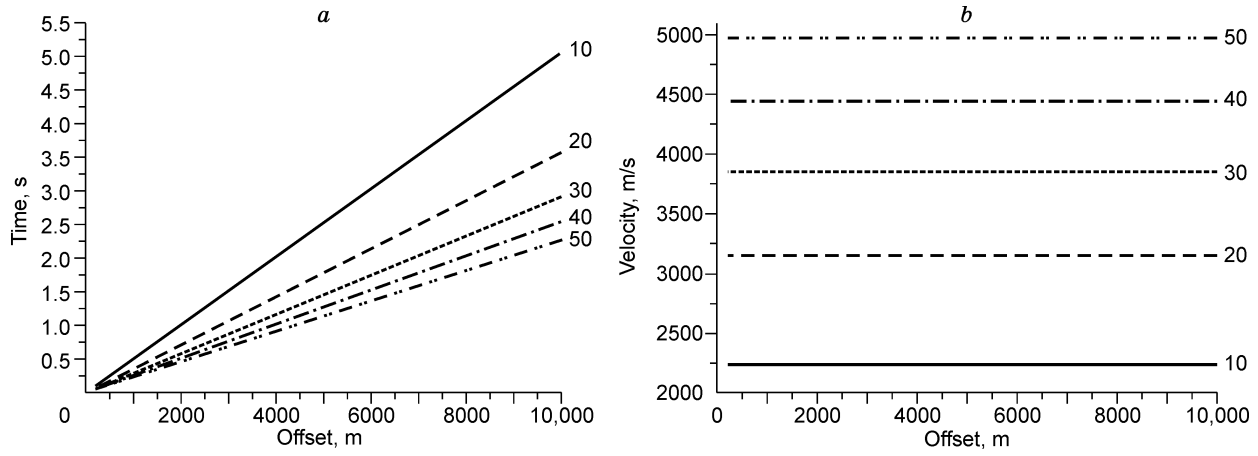

Fig. 6. Travel times of wave transforms for the conductive half-space (*a*), velocity curves derived from wave transforms for the conducitng half-space (*b*). Curves show resistivity, in Ohm·m.

horizontal plate with the conductivity $S = \lim_{h\to 0,\ \rho\to 0} h/\rho$, at the depth z in a nonconductive homogeneous space (h and ρ are, respectively, the thickness and resistivity of a single conductor in a nonconductive medium). For a coductor, the time deconvolution of voltage is given by (Sidorov, 1985)

$$\frac{\partial B_z}{\partial t} = \frac{Mq}{\pi S}\frac{m[3r^2 - 8m^2]}{[r^2 + 4m^2]^{7/2}},$$

where $m = z + t/\mu S$; q is the moment of the receiver loop (dot product of its surface and number of turns); r is the offset (distance from the source to the receiver center).

For numerical transformation of the signal into the wave domain, consider a 10 m thick conductive layer, with the conductivity S (10, 20, 50, 100 S/m) in a non-conductive medium. The layer top lies at the depth z_1 = 10 m. A transmitter and 30 receivers lie along the same line with the offsets from 150 to 400 m. The velocity calculated after the transformation (Fig. 7) decerases when conductivity S increases while the velocity ratio v_1/v_2 is $\sqrt{S_2/S_1}$.

All travel-time curves at a resistivity varying from 10 to 60 Ohm·m in the first layer of the three-layer model (Fig. 8*a*) converge at one point at short offsets, and their slope is inversely proportional to resistivity. The time difference is greater at larger offsets and reaches 1.58 s at r = 10,000 m. The velocity of the wave transform increases with resistivity (Fig. 8*b*), from 2000 to 5000 m/s at short offsets and within 4900–9500 m/s at long offsets.

Travel times of the fictitious wave increase ($\Delta t = 0.22$ s, r = 10,000 m) as ρ_2 becomes ten times greater (Fig. 9*a*). At offsets shorter than 2200 m, travel times are almost independent of the resistivity of the second layer. The respective velocities of the wave transform (Fig. 9*b*) increase with the resistivity of the second layer at offsets longer than 2200 m.

Travel times depend also on the thickness of the conductor (Fig. 10*a*): travel-time curves almost coinside at offsets less than 3200 m and then increase with layer thickness; Δt reaches 1.59 s at 10,000 m. The velocity patterns derived from travel times (Fig. 10*b*) show almost no offset dependence at large h_1, with the velocity about 2095–2230 m/s. As h_1 decreases, the velocity changes more strongly: 2230–3560 m/s at h_1 = 2000 m; 2230–4900 m/s at h_1 = 1000 m.

Conclusions

TEM data can be transformed into the wave-equation domain using the SVD or Tikhonov regularizations. Special techniques have been suggested to calculate travel times and velocities of the respective wave transforms. The tested earth models include a half-space, a thin conductor in a non-conducting space (**S** film), and a layered half-space with two plane-parallel boundaries. The velocity-resistivity relationships obtained for models of a homogeneous conducting half-space and a thin condutor are $V_1/V_2 = \sqrt{\rho_1/\rho_2}$.

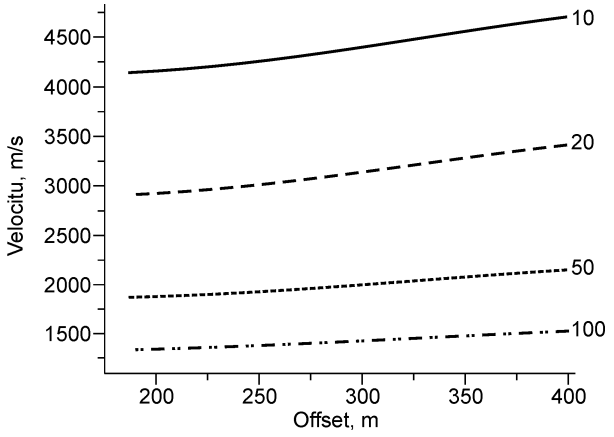

Fig. 7. Velocity curves derived from wave transforms of the conducting *S* film. Curves show conductivity of *S* film, in S/m.

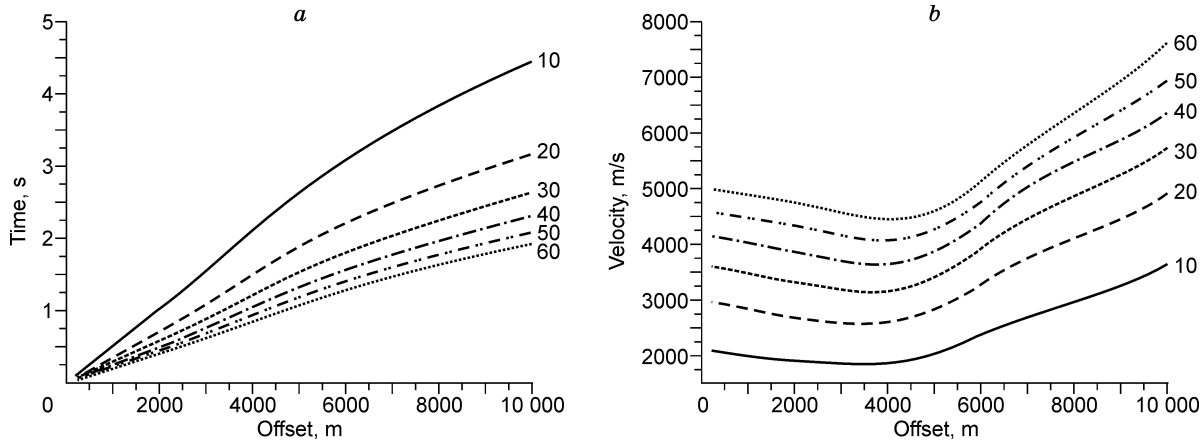

Fig. 8. Travel times as a function of resistivity of the first layer (*a*) and velocity derived from wave transforms as a function of resistivity of the first layer in a three-layer earth (model 1) (*b*). Curves show resistivity: ρ_1 = 10, 20, 30, 40, 50 Ohm·m.

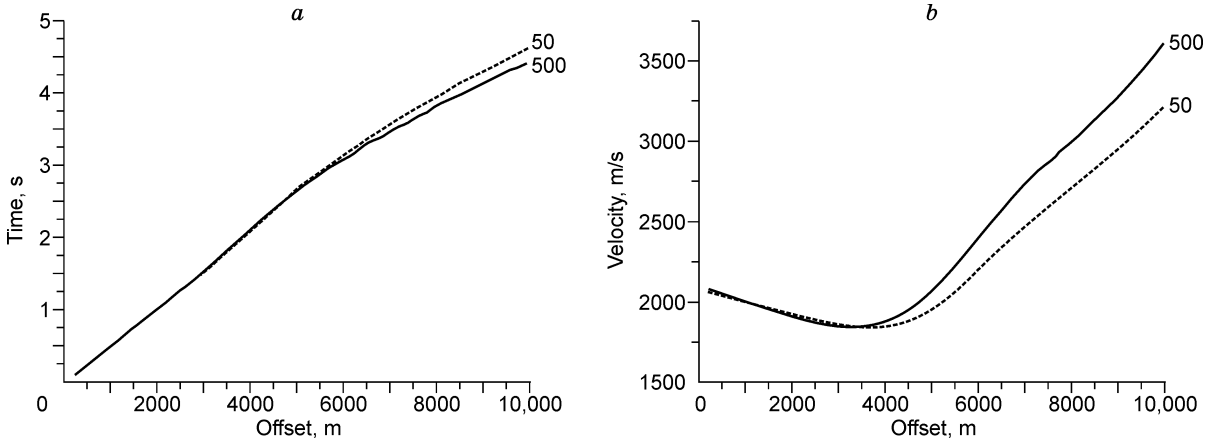

Fig. 9. Travel times as a function of resistivity of the second layer (*a*) and velocity derived from wave transforms as a function of resistivity of the second layer in a three-layer earth (model 1) (*b*). Curves show resistivity: ρ_1 = 50, 500 Ohm·m.

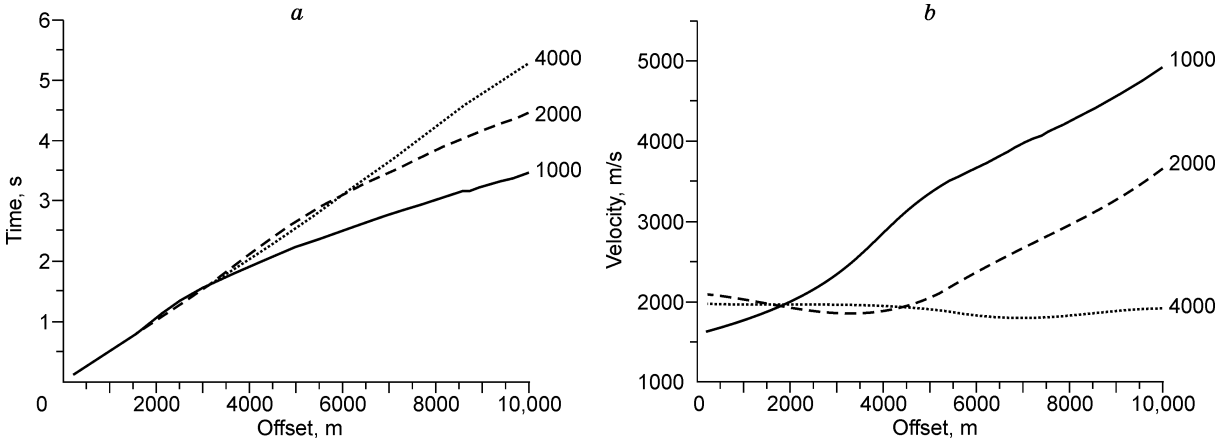

Fig. 10. Travel times as a function of thickness of the first layer (*a*) and velocity derived from wave transforms as a function of thickness of the first layer in a three-layer earth (model 1) (*b*). Curves show layer thickness: h_1 = 1000, 2000, 4000 m.

References

Hoop, A.T., 1996. A general correspondence principle for time-domain electromagnetic wave and diffusion fields. Geophys. J. Int. 127, 757–761.

Gershenson, M., 1997. Simple interpretation of time-domain electromagnetic sounding using similarities between wave and diffusion propagation. Geophysics 62, 763–774.

Gibert, D. Virieux, J., 1991. Electromagnetic imaging and simulated annealing. J. Geophys. Res. 96, 8057–8067.

Kamenetsky, F.M., 1997. Geophysical Surveys by Transient Electromagnetic Soundings [in Russian]. GEOS, Moscow.

Kaufman, A.A., Morozova, G.M., 1970. Transient Electromagnetic Soundings: Theoretical Background [in Russian]. Nauka, Novosibirsk.

Kunetz, G., 1972. Processing and interpretation of magnetotelluric soundings. Geophysics 37, 1005–1021.

Lee, K.H., Xie, G., 1993. A new approach to imaging with low-frequency electromagnetic fields. Geophysics 58, 780–796.

Lee, K.H., Liu, G., Morrison, H.F., 1989. A new approach to modeling the electromagnetic response of conductive media. Geophysics 54, 1180–1192.

Levy, S., Oldenburg, D., Wang, J., 1988. Subsurface imaging using magnetotelluric data. Geophysics 53, 104–117.

Mittet, R., 2015. Seismic wave propagation concepts applied to the interpretaion of marine controlled-source electromagnetics. Geophysics 80, 63–81

Nekut, A.G., 1994. Electromagnetic ray-trace tomography. Geophysics 59, 371–377.

Reznitskaya, K.G., 1974. Relation between Cauchy solutions for equations of different types and inversion, in: Mathematical Problems of Geophysics [in Russian]. Computing Center, USSR Academy of Sciences, Novosibirsk, Issue 5 (I), pp. 55–62.

Sheinmann, S.M., 1969. Theory of Resistivity Surveys: Modern Physical Background [in Russian]. Nedra, Moscow.

Sidorov, V.A., 1985. Pulse Induction Resistivity Soundings [in Russian]. Nedra, Moscow.

Slob, E.C., Habashy, T.M., Torres-Verdin, C., 1995. A new stable numerical procedure for computing the q-transform of TEM data, in: Proc. EAGE 57th Conference and Technical Exhibition, Glasgow, Scotland, pp. 221–223.

Swidinsky, A., 2011. Transient Electromagnetic Modelling and Imaging of Thin Resistive Structures: Applications for Gas Hydrate Assessment. A thesis submitted in conformity with the requirements for the degree of Doctor of Philosophy Department of Physics, University of Toronto.

Tikhonov, A.N., Arsenin, V.Ya., 1979. Methods for Solving Ill-posed Problems, second ed. [in Russian]. Nauka, Moscow.

Van'yan, L.L., 1963. Resistivity Surveys by Transient Electromagnetic Soundings [in Russian]. Gosgeoltekhizdat, Moscow.

Van'yan, L.L., 1965. Fundamentals of Electromagnetic Soundings [in Russian]. Nedra, Moscow.

Virieux, J., Flores-Luna, C., Gibert, D., 1994. Asymptotic theory for diffusive electromagnetic imaging. Geophys. J. Int. 119, 857–868.

Weidelt, P., 1972. The inverse problem of geomagnetic induction. Zeit. für Geophys. 38, 257–298.

Wilson, A.J.S., 1994. Seismic processing of multichannel transient electromagnetic (MTEM) data, in: Proc. EAGE 56th Conference and Technical Exhibition, Vienna, Austria, pp. 123–124.

Xie, G., Bai, C., Li, X., 2012. Extracting the virtual reflected wavelet from TEM data based on regularizing method. Pure Appl. Geophys. 169, 1269–1282.

Yu, L., Edwards, R.N., 1997. On crosswell diffusive time-domain electromagnetic tomography. Geophys. J. Int. 130, 449–459.

Zhdanov, M.S., Frenkel, M.A., 1983. The solution of the inverse problems on the basis of the analytical continuation of the transient electromagnetic field in reverse time. J. Geomag. Geoelectr. 35, 747–765.

Editorial responsibility: A.D. Duchkov